

# Manifestation of ferroelectromagnetism in multiferroic BiMnO<sub>3</sub>

Z. H. Chi, C. J. Xiao, S. M. Feng, F. Y. Li, and C. Q. Jin<sup>a)</sup>

*Institute of Physics, Chinese Academy of Sciences, Beijing 100080, People's Republic of China*

X. H. Wang, R. Z. Chen, and L. T. Li

*State Key Laboratory of New Ceramics and Fine Processing, Department of Materials Science and Engineering, Tsinghua University, Beijing 100084, People's Republic of China*

(Received 24 June 2005; accepted 10 October 2005; published online 23 November 2005)

Multiferroic BiMnO<sub>3</sub> with a highly distorted perovskite structure induced by the stereochemically active  $6s^2$  electron lone pairs of Bi<sup>3+</sup> was synthesized at a high pressure of 6 GPa. Magnetization, differential scanning calorimetry, dielectric permittivity, and *in situ* powder x-ray diffraction as a function of temperature were carried out, respectively. In light of comprehensive evaluation, we can conclude that the synthetic BiMnO<sub>3</sub> ceramic displays ferromagnetic and ferroelectric orderings simultaneously, i.e., ferroelectromagnetism below its ferromagnetic Curie temperature  $T_M \sim 100$  K. © 2005 American Institute of Physics. [DOI: [10.1063/1.2131193](https://doi.org/10.1063/1.2131193)]

## I. INTRODUCTION

Multiferroic compounds in which two or all three ferroic order parameters, i.e., spontaneous polarization, spontaneous magnetization, and spontaneous strain coexist in the same phase,<sup>1</sup> have gained renewed and ever increasing research interest during the past several years.<sup>2-6</sup> In particular, those wherein magnetic and ferroelectric orderings occur simultaneously, termed ferroelectromagnet,<sup>7</sup> an intrinsic coupling between magnetic and ferroelectric sublattices would come into play, in addition to pristine spontaneous magnetization and polarization. As a result, nontrivial magnetoelectric (ME) effect, i.e., induction of electric polarization by means of magnetic field and/or vice versa in ferroelectromagnet is expected, thus offering a degree of freedom in device designing. Besides the enormous potential applications in information storage devices based on the reversal of either electric polarization or magnetic polarization vector, wherein binary byte (0 and 1) can be written in the form of either polarization vector and read out by magnetic and/or electric field, in addition, both polarization vectors are coupled together and easy to be manipulated via a tiny perturbation such as electric and/or magnetic field in the vicinity of concurrent phase-transition temperature. The fundamental physics mechanism behind multiferroic is rich and fascinating to be exploited. Although investigation on ferroelectromagnet can be traced back to 1950s,<sup>8</sup> the renaissance of this class of materials was just heralded by the discovery of the so-called colossal magnetodielectric (MD) or magnetocapacitance (MC) effect in rare-earth manganite,<sup>2-6</sup> signaling a robust interplay between magnetic and dielectric properties. Very recently, BiMnO<sub>3</sub> (BMO) was unraveled to be a supplement to the scarce multiferroic family, in which MC via ME effect has been evidenced.<sup>9</sup> An intriguing peculiarity of BiMnO<sub>3</sub> lies in that it can only be synthesized in bulk form by resorting to high pressures of at least 3 GPa.<sup>10</sup> For two-dimensional (2D) thin-film architecture, the gigantic stress generated in the film-

substrate interface can stabilize the distorted perovskite structure caused by lone pair, as demonstrated in multiferroic BiFeO<sub>3</sub> thin film.<sup>11</sup> Once quenched to ambient environment, the bulk BiMnO<sub>3</sub> survives as a metastable phase. This renders it hard to be synthesized, especially for a well-shaped single crystal. As far as magnetism is concerned, it has been well established that BiMnO<sub>3</sub> becomes ferromagnetically ordering upon cooling below 103 K,<sup>12</sup> in sharp contrast with homologous rare-earth manganites  $ReMnO_3$  ( $Re=La-Lu$ ) ordering antiferromagnetically below the respective Neel temperature  $T_N$ . As for room-temperature crystal structure and dielectric property, BiMnO<sub>3</sub> is monoclinic and ferroelectric;<sup>7,9</sup> in contrast, light rare-earth manganites  $ReMnO_3$  ( $Re=La-Dy$ ) are orthorhombic and nonferroelectric, whereas, the heavy ones  $ReMnO_3$  ( $Re=Y, Ho-Lu$ ) are hexagonal and ferroelectric. It is noteworthy here that Bi<sup>3+</sup> and  $Re^{3+}$  ions are very similar both in valence state and ionic radius. These striking distinctions in both structure and physical properties between BiMnO<sub>3</sub> and  $ReMnO_3$  have been elaborated by Hill<sup>13</sup> through first-principles calculation. They pointed out that the  $6s^2$  electron lone pairs of Bi<sup>3+</sup> plays a crucial role in stabilizing different magnetic and structural characteristics in BiMnO<sub>3</sub> compared with rare-earth manganites. Another feature of their calculation is to elucidate the origin of dearth in coexistence between ferroelectricity and magnetism, suggesting that unpaired transition-metal  $d$  electron which is a prerequisite for magnetism reduces the tendency for off-center ferroelectric distortion. Detailed information concerning BiMnO<sub>3</sub> has been garnered, including the polar monoclinic structure (space-group  $C2$ ) of ferroelectric phase,<sup>14</sup> ferromagnetism, ferroelectricity, and possible coexistence below a certain temperature<sup>15</sup> during the last decades. In comparison with its intimate neighbors BiCrO<sub>3</sub> (BCO) and BiFeO<sub>3</sub> (BFO) in Periodic Table [the former is both ferroelectric ( $T_E=440$  K) and parasitic ferromagnetic ( $T_N=114$  K)],<sup>12,16</sup> the latter is both ferroelectric ( $T_E=1123$  K) and antiferromagnetic ( $T_N=650$  K) (Ref. 7) accompanied by weak ferromagnetism due to spin canting at room temperature], BiMnO<sub>3</sub> [ferroelectric ( $T_E=450$  or 750 K) and ferro-

<sup>a)</sup>Author to whom correspondence should be addressed; electronic mail: [cqjin@aphy.iphy.ac.cn](mailto:cqjin@aphy.iphy.ac.cn)

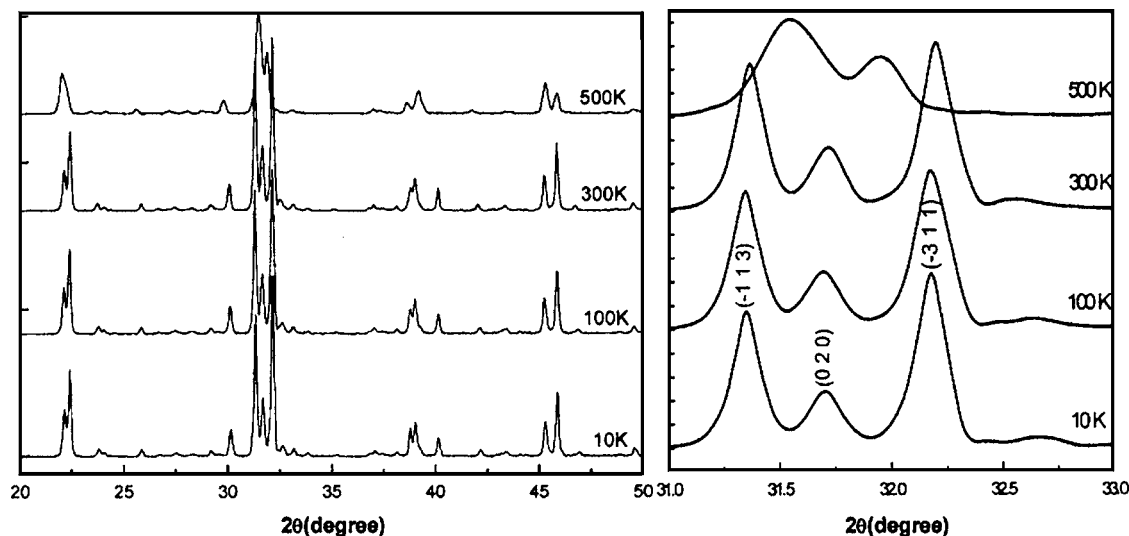


FIG. 1. Portion of variable-temperature powder XRD pattern of synthetic BMO ceramic. [The left panel is the region between  $20^\circ$  and  $50^\circ$  in  $2\theta$  showing all strong reflection peaks; the right is the local amplification between  $31^\circ$  and  $33^\circ$  highlighting the amalgamation of  $(-113)$ ,  $(020)$ , and  $(-311)$  peaks.]

magnetic ( $T_M=103$  K) (Refs. 7, 9, 12, and 15) is more affinitive with the former taking into account an identical monoclinic ( $C2$ ) structure at room temperature.<sup>16</sup> Moreover, many researchers have been dedicated to the fabrication of BMO thin film for integration of electronic devices with potential multifunctionalities.<sup>17–19</sup> The goal of this paper is to comprehensively corroborate the ferroelectromagnetic nature of  $\text{BiMnO}_3$  ceramic fabricated at high pressures and enumerate several articles of fundamental parameters, which may pave the way for expected applications.

## II. EXPERIMENT

Polycrystalline  $\text{BiMnO}_3$  ceramic was fabricated under high pressures utilizing a cubic-anvil-type high-pressure apparatus. The starting reagent  $\text{Mn}_2\text{O}_3$  was calcined at 1000 K in air for several days to obtain appropriate valence. Stoichiometric mixture of  $\text{Bi}_2\text{O}_3$  and  $\text{Mn}_2\text{O}_3$  was ground intimately in an agate mortar followed by calcination in alumina crucible at 600 K for 24 h to enable the preliminary reaction between  $\text{Mn}_2\text{O}_3$  and  $\text{Bi}_2\text{O}_3$ . The calcined mixture was finely ground again and pressed into a cylinder ( $\varphi 5$  mm in diameter  $\times$  2 mm in height) and encapsulated in silver foil to prevent contamination. Afterwards, the capsule was pressed in the center of a NaCl cylinder ( $\varphi 8$  mm in diameter  $\times$  15 mm in height), serving as pressure and heat-transmitting medium. Ultrafine NaCl powder has proven to be more efficient in keeping excellent quasihydrostatic pressure. Finally, the NaCl cylinder nested in a tubular graphite heater was introduced into a pyrophyllite cube and subjected to 6 GPa and 1173 K for 30 min. Pressure was released slowly after quenching the specimen to room temperature. The x-ray-diffraction (XRD) pattern was recorded by M18AHF diffractometer (MAC SCIENCE, Japan) employing  $\text{Cu } K\alpha$  radiation to identify the phase purity. Analysis of the XRD pattern indicated that the main phase could be indexed on the basis of a monoclinic unit cell with  $C2$  (No. 5) space group at room temperature. However, a trace amount of contaminant phases including  $A\text{-Bi}_2\text{O}_3$  and

$\text{Bi}_2\text{O}_2\text{CO}_3$  was included in the final specimen in spite of much effort made to improve specimen purity. The former is a high-pressure derivative of  $\text{Bi}_2\text{O}_3$  stabilized at 6 GPa which can be quenched to ambient condition. The latter is produced as a result of  $\text{CO}_2$  contamination released from graphite heater. Both impurity phases are nonmagnetic and ordinary dielectrics. Their contributions to the ferroelectricity and ferromagnetism of the final specimen are negligible. Variable-temperature XRD was carried out between the temperature range of 10 and 500 K to follow the possible temperature-dependent structural evolution. Magnetization measurement was performed at commercial Maglab physical property measuring system (Oxford Instruments). Differential scanning calorimetry (DSC) scanning was conducted from room temperature up to 870 K with a heating rate of 10 K/min. Meticulous caution was taken to prevent specimen from oxidation by means of flowing Ar atmosphere during heating process. For dielectric properties test, specimen was transformed into a thin plate with smooth faces onto which Au electrodes were evaporated in vacuum. Dielectric permittivity measurement was conducted on a HP 4294A impedance analyzer up to 823 K, which precedes the decomposition of  $\text{BiMnO}_3$  at about 873 K. Specimen was heated in flowing  $\text{N}_2$  ambience to prevent oxidation during the measuring process.  $I$ - $V$  curve characterization was performed on TF analyzer 2000 ferroelectric tester.

## III. RESULTS AND DISCUSSION

Variable-temperature powder XRD pattern was recorded by  $\text{Cu } K\alpha$  radiation in the temperature range of 10–500 K. Data processing and structure refinement were performed employing POWDER X software packet.<sup>20</sup> It is evident in Fig. 1 that the crystal structure at 10 K is the same as that at room temperature, indicating that no structural phase transition occurs upon cooling the polar structure at room temperature through ferromagnetic Curie temperature down to 10 K, lending support to the belief that ferromagnetism and ferroelectricity coexist in  $\text{BiMnO}_3$  below the ferromagnetic Curie

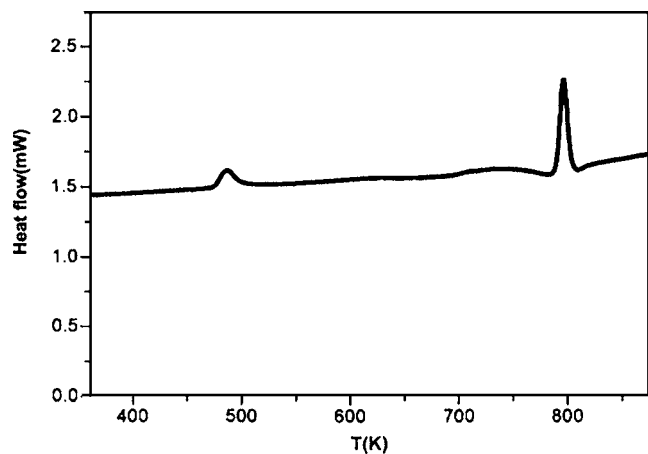


FIG. 2. Temperature dependence of the heat flow of BMO ceramic measured by DSC scanning. (The former endothermic peak corresponds to the transition between two ferroelectric phases; the latter peak corresponds to the transition from ferroelectric to paraelectric phase.)

temperature. In contrast, the structure at 500 K is significantly distinct from that at low temperatures, reflecting a structural transition to higher symmetry indicated by the amalgamation of diffraction peaks in the interval between  $31^\circ$  and  $33^\circ$  in  $2\theta$ . This structural transition was foremost reported by Sugawara *et al.* in their groundbreaking work on  $\text{BiMnO}_3$ ,<sup>12</sup> wherein they characterized it to be a transition between two pseudotriclinic phases with slight changes in distortion mode. Contemporary researchers in the USSR deemed that this transition was in relation to a slight change of the superstructure.<sup>21</sup> From the viewpoint of Kimura *et al.*,<sup>9</sup> this distinction can be interpreted to be a first-order structural phase transition between two monoclinic ferroelectric phases. On the contrary, Moreira dos Santos *et al.*<sup>15</sup> ascribed the structural phase transition around 500 K to be a reversible and second-order monoclinic ferroelectric to monoclinic paraelectric phase transition. As mentioned above,<sup>16</sup> BMO and BCO adopt the same monoclinic ( $C2$ ) structure at room temperature and neighboring ferroelectric Curie temperature  $T_E$ , thus we can postulate that they adopt identical paraelectric phase structure, i.e., orthorhombic ( $Pnma$ ) at around 500 K, as a result of similar ionic radius of  $\text{Mn}^{3+}$  and  $\text{Cr}^{3+}$ . From the diffraction data analysis based on POWDER X software packet, our BMO specimen gives a similar solution for  $C2$  monoclinic and  $Pnma$  orthorhombic structures due to a subtle distortion relationship.

It is generally accepted that ferroelectric phase transition is a typical structural phase transition in nature. To intuitively discern plausible structural phase transition, thermal analysis has proven to be a convenient avenue. Figure 2 shows the DSC profile of synthetic  $\text{BiMnO}_3$  ceramic. There are two outstanding endothermic peaks around 470 and 770 K, corresponding to two structural transitions. In the opinion of Kimura *et al.*,<sup>9</sup> the former is related to a transition between two monoclinic ferroelectric phases, the latter is related to a transition to  $Pbnm$  orthorhombic paraelectric phase. The latter transition temperature coincides well with the ferroelectric Curie temperature of  $\text{BiMnO}_3$  at 773 K reported in literature.<sup>7</sup> However, Moreira dos Santos *et al.* described the latter to be a irreversible transition with composition

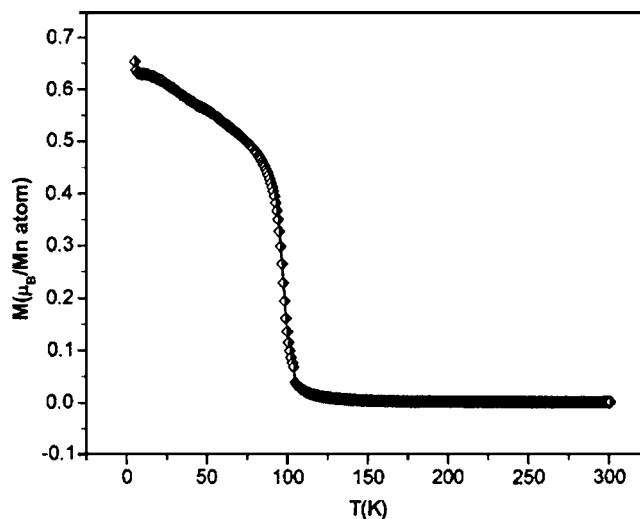


FIG. 3. Temperature dependence of the magnetization of synthetic BMO ceramic. (The specimen was cooled in zero field and measured with an applied field of 1000 G from 5 up to 300 K.)

change.<sup>15</sup> Faqir *et al.* assigned the latter to be a transition from triclinic to tetragonal<sup>22</sup> just preceding the decomposition temperature of 873 K. Until now, the crystal structure of high-temperature paraelectric phase is still of controversy.

As demonstrated in Fig. 3, magnetization measurement on  $\text{BiMnO}_3$  ceramic at an applied magnetic field of 0.1 T manifests ferromagnetism with a Curie temperature close to 100 K, in good agreement with published data. It has been evidenced that ferromagnetism in  $\text{BiMnO}_3$  stems from a particular orbital ordering of  $e_g$  electrons on  $\text{Mn}^{3+}$  ion.<sup>23</sup> Figure 4 presents the  $M$ - $H$  hysteresis loop measured at 5 K. The calculated magnetic moment of  $\text{Mn}^{3+}$  is  $2.83\mu_B$  at 1 T and 5 K, which is smaller than the fully aligned spin value of  $4\mu_B$  for  $\text{Mn}^{3+}(3d^4)$ . To account for this remarkable difference, a distorted Mn-O-Mn superexchange pathway as a result of cooperation between Jahn-Teller effect of  $\text{Mn}^{3+}$  and lone pair effect of  $\text{Bi}^{3+}$  should be taken into consideration. From the  $M$ - $H$  hysteresis loop, we can extrapolate the coercive field of 0.02 T and remnant magnetization of  $0.2\mu_B$  at 5 K, indicating a weakly ferromagnetic behavior of  $\text{BiMnO}_3$ .

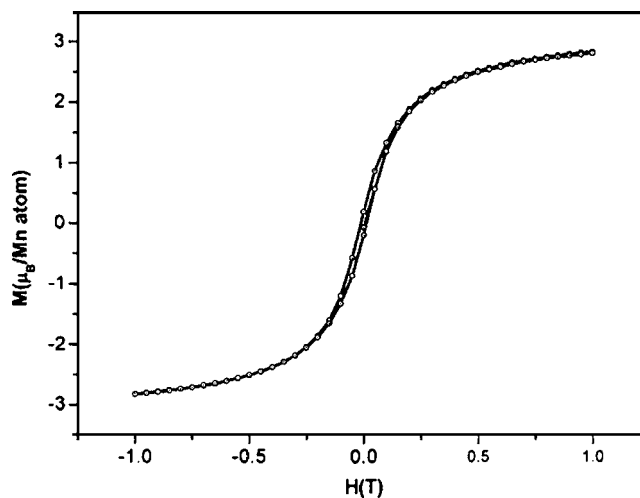


FIG. 4.  $M$ - $H$  hysteresis loop of synthetic BMO ceramic measured with an applied field of 1 T at 5 K.

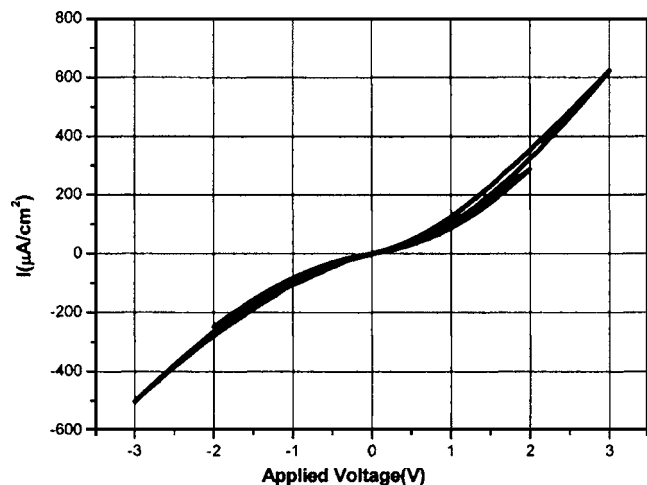


FIG. 5.  $I$ - $V$  curve of thin plate BMO ceramic at applied voltages of 2 and 3 V, respectively.

Attempt to acquire a well-defined  $P$ - $E$  hysteresis loop fell through due to a significant electrical avalanche on applying a relatively low voltage to the chip-configuration capacitor made of as-prepared BMO ceramic. This conundrum has been encountered in many kinds of perovskite ferroelectric ceramics<sup>24</sup> for a long time. The mechanism inducing leakage current in BMO ceramic can be attributed to ion vacancy (denoted as  $V_{\text{O}}^{2+}$  or  $V_{\text{Bi}}^{3-}$ ), conducting impurity, defect, or nonstoichiometry in the sample. It is well known that in Colossal Magnetoresistance (CMR) manganite  $\text{La}(\text{Ca}, \text{Sr})\text{MnO}_3$  (LSMO or LCMO), a double-exchange interaction between  $\text{Mn}^{3+}$  and  $\text{Mn}^{4+}$  makes it highly conductive. Strictly speaking, for stoichiometric  $\text{BiMnO}_3$  accommodating pure  $\text{Mn}^{3+}$ , it should be a robust insulator like end member  $\text{LaMnO}_3$  of CMR manganite. But when we take into consideration the purity of starting  $\text{Mn}_2\text{O}_3$  (98%, Alfa Aesar), it is not surprising that a trace amount of  $\text{Mn}^{4+}$  in the final specimen makes the double-exchange pathway feasible; consequently, the accumulation of charge carrier makes  $\text{BiMnO}_3$  semiconductor like. Another mechanism is pertinent to ion vacancy including  $V_{\text{O}}^{2+}$  or  $V_{\text{Bi}}^{3-}$ . Due to high volatility of  $\text{Bi}_2\text{O}_3$ , the final product may be  $\text{Bi}^{3+}$  deficient, thus generates  $V_{\text{Bi}}^{3-}$  in lattice accompanied by the emergence of  $V_{\text{O}}^{2+}$ . Both  $V_{\text{Bi}}^{3-}$  and  $V_{\text{O}}^{2+}$  vacancies are highly mobile and inclined to induce leakage current on the application of electric field. The final mechanism is speculated to arise from a metastable  $\text{A}-\text{Bi}_2\text{O}_3$  impurity quenched from high temperatures and high pressures, which shows high ion conductivity due to high mobility of  $\text{O}^{2-}$  ions.<sup>25</sup> Figure 5 depicts the  $I$ - $V$  relationship of a thin plate BMO ceramic measured with an upper limit of applied voltage up to 2 and 3 V, respectively. The current density reached an extraordinarily giant value on applying a very low voltage, indicating a high order of leakage behavior. In view of the semiconductorlike behavior, further  $P$ - $E$  loop measurement is to be conducted far below room temperature to enhance the resistivity of specimen. In the literatures so far, only one paper has reported a well-saturated  $P$ - $E$  loop in imperfect bulk and thin-film  $\text{BiMnO}_3$ .<sup>15</sup> Convincing and definitive evidence to ascertain ferroelectricity in  $\text{BiMnO}_3$  is still elusive to us due to the

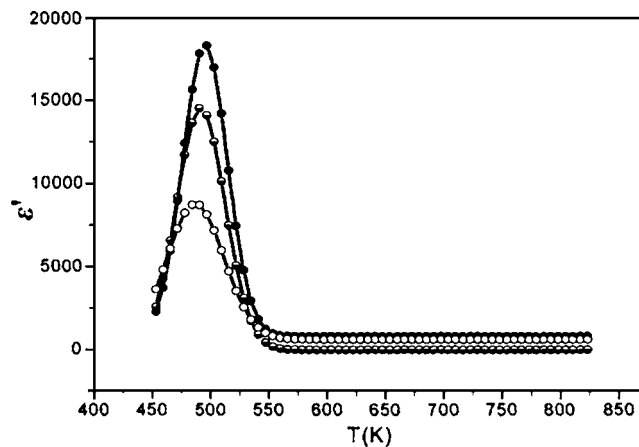


FIG. 6. Temperature dependence of dielectric permittivity of synthetic BMO ceramic measured at different frequency. (The filled, half-filled, and open circle represent experimental data measured at 40, 1000, and 10 000 Hz, respectively.)

difficulty in growing single-crystalline  $\text{BiMnO}_3$ . To circumvent a severe leakage current in bulk form, some researchers have turned to other techniques as optical second-harmonic generation (SHG) to detect ferroelectricity in  $\text{BiMnO}_3$  thin film indirectly.<sup>26</sup>

Up to now, no report on dielectric permittivity measurement of  $\text{BiMnO}_3$  was documented in published literatures for unknown reason. In the course of our research, dielectric permittivity ( $\epsilon'$ ) measurement unveiled relaxorlike ferroelectricity in  $\text{BiMnO}_3$ , as shown in Fig. 6. It should be noted here that the original data were fitted with a Gaussian function. A pronounced divergence in  $\epsilon'$  appears in the vicinity of 500 K, corresponding to the transition between two ferroelectric phases indicated in Ref. 9 or ferroelectric-paraelectric transition indicated in Ref. 15. However, in conventional ferroelectric like  $\text{BaTiO}_3$  (BTO), only a minute fluctuation in  $\epsilon_r$  emerges across the transition between two ferroelectric phases. Otherwise, the transition around 500 K may be interpreted to be a ferroelectric-paraelectric transition suggested by Moreira dos Santos *et al.*<sup>15</sup> The magnitude of  $\epsilon'$  diminishes with increasing frequency. A slight shift to lower temperature with increasing frequency in the phase-transition temperature is readily detected. No explicit anomaly in dielectric permittivity was discerned around the ferroelectric-paraelectric transition temperature close to 770 K proposed in literature.<sup>7,9</sup> This is likely to be attributed to the enhanced conductivity of specimen at higher temperature. Further measurement is to be conducted in oxygen atmosphere for the sake of suppressing oxygen vacancy conduction.

#### IV. CONCLUSION

In summary, multiferroic  $\text{BiMnO}_3$  (BMO) ceramic has been fabricated under high-pressure and high-temperature conditions. Ferroelectromagnetism of  $\text{BiMnO}_3$  has been comprehensively verified via magnetization, temperature-dependent dielectric permittivity scanning, thermal analysis, and variable-temperature powder x-ray diffraction. Effort to make synthetic  $\text{BiMnO}_3$  ceramic a robust insulator via alio-



valent ions doping or annealing in high oxygen-pressure ambience to sustain higher applied voltage is in progress.

## ACKNOWLEDGMENTS

This work was financially sponsored by Natural Science Foundation and Ministry of Science and Technology of China through the research projects (50321101, 50332020, 5041009, and 2002CB613301). The authors are grateful to Professor J. S. Zhou for the inspired discussions.

<sup>1</sup>H. Schmid, *Ferroelectrics* **162**, 317 (1994).

<sup>2</sup>N. Hur, S. Park, P. A. Sharma, S. Guha, and S.-W. Cheong, *Phys. Rev. Lett.* **93**, 107207 (2004).

<sup>3</sup>L. C. Chapon, G. R. Blake, M. J. Gutmann, S. Park, N. Hur, P. G. Radaelli, and S.-W. Cheong, *Phys. Rev. Lett.* **93**, 177402 (2004).

<sup>4</sup>M. Fiebig, Th. Lottermoser, D. Frohlich, A. V. Goltsev, and R. V. Pisarev, *Nature (London)* **419**, 818 (2002).

<sup>5</sup>T. Kimura, T. Goto, H. Shintani, K. Ishizaka, T. Arima, and Y. Tokura, *Nature (London)* **426**, 55 (2003).

<sup>6</sup>Th. Lottermoser, Th. Lonkai, U. Amann, D. Hohlwein, J. Ihringer, and M. Fiebig, *Nature (London)* **430**, 541 (2004).

<sup>7</sup>G. A. Smolenskii and I. E. Chupis, *Sov. Phys. Usp.* **25**, 475 (1982).

<sup>8</sup>G. A. Smolenskii, A. I. Agranovskaya, S. N. Popov, and V. A. Isupov, *Zh. Tekh. Fiz.* **28**, 2152 (1958) [*Sov. Phys. Tech. Phys.* **3**, 1981 (1958)].

<sup>9</sup>T. Kimura, S. Kawamoto, I. Yamada, M. Azuma, M. Takano, and Y. Tokura, *Phys. Rev. B* **67**, 180401(R) (2003).

<sup>10</sup>F. Sugawara, S. Ihda, Y. Syono, and S. Akimoto, *J. Phys. Soc. Jpn.* **20**, 1529 (1965).

<sup>11</sup>J. Wang, *et al. Science* **299**, 1719 (2003).

<sup>12</sup>F. Sugawara, S. Ihda, Y. Syono, and S. Akimoto, *J. Phys. Soc. Jpn.* **25**, 1553 (1968).

<sup>13</sup>N. A. Hill, *J. Phys. Chem. B* **104**, 6694 (2000).

<sup>14</sup>T. Atou, H. Chiba, K. Ohoyama, Y. Yamaguchi, and Y. Syono, *J. Solid State Chem.* **145**, 639 (1999).

<sup>15</sup>A. Moreira dos Santos, S. Parashar, A. R. Raju, Y. S. Zhao, A. K. Cheetham, and C. N. R. Rao, *Solid State Commun.* **122**, 49 (2002).

<sup>16</sup>S. Niitaka, M. Azuma, M. Takano, E. Nishibori, M. Takata, and M. Sakata, *Solid State Ionics* **172**, 557 (2004).

<sup>17</sup>A. Moreira dos Santos, A. K. Cheetham, W. Tian, X. Q. Pan, Y. F. Jia, N. J. Murphy, J. Lettieri, and D. G. Schlom, *Appl. Phys. Lett.* **84**, 91 (2004).

<sup>18</sup>J. Y. Son, B. G. Kim, C. H. Kim, and J. H. Cho, *Appl. Phys. Lett.* **84**, 4971 (2004).

<sup>19</sup>A. Sharan, I. An, C. Chi, R. W. Collins, J. Lettieri, Y. Jia, D. G. Schlom, and V. Gopalan, *Appl. Phys. Lett.* **83**, 5169 (2003).

<sup>20</sup>C. Dong, *J. Appl. Crystallogr.* **32**, 838 (1999).

<sup>21</sup>Y. Y. Tomashpol'skii, E. V. Zubova, K. P. Burdina, and Y. N. Venetsev, *Izv. Akad. Nauk SSSR, Neorg. Mater.* **3**, 2132 (1967).

<sup>22</sup>H. Faqir, H. Chiba, M. Kikuchi, and Y. Syono, *J. Solid State Chem.* **142**, 113 (1999).

<sup>23</sup>A. Moreira dos Santos, A. K. Cheetham, T. Atou, Y. Syono, Y. Yamaguchi, K. Ohoyama, H. Chiba, and C. N. Rao, *Phys. Rev. B* **66**, 064425 (2002).

<sup>24</sup>A. K. Pradhan, *et al. J. Appl. Phys.* **97**, 093903 (2005).

<sup>25</sup>T. Atou, H. Faqir, M. Kikuchi, H. Chiba, and Y. Syono, *Mater. Res. Bull.* **33**, 289 (1998).

<sup>26</sup>A. Sharan, J. Lettieri, Y. F. Jia, W. Tian, X. Q. Pan, D. G. Schlom, and V. Gopalan, *Phys. Rev. B* **69**, 214109 (2004).